SAND--82-0793C

DE82 017024

NATURAL-CONVECTION EXPERIMENTS IN A LIQUID-SATURATED POROUS MEDIUM BOUNDED BY VERTICAL COAXIAL CYLINDERS*

by

Daniel C. Reda
Fluid and Thermal Sciences Department
Sandia National Laboratories
Albuquerque, NM 87185

Submitted for Presentation at

ASME-JSME THERMAL ENGINEERING JOINT CONFERENCE
Honolulu, Hawaii
March 20-24, 1983

*This work performed at Sandia National Laboratories supported by the U. S. Department of Energy under Contract Number DE-AC04-76DP00789.

DISCLAIMER

NATURAL-CONVECTION EXPERIMENTS IN A LIQUID-SATURATED POROUS MEDIUM BOUNDED BY VERTICAL COAXIAL CYLINDERS†

by

Daniel C. Reda*
Fluid and Thermal Sciences Department
Sandia National Laboratories
Albuquerque, NM 87185

ABSTRACT

An experimental effort is presently underway to investigate natural convection phenomena in liquid-saturated porous media utilizing a geometry, and hydrodynamic/thermal boundary conditions, relevant to the problem of nuclear-waste isolation in geologic repositories. During the first phase of this research program, detailed measurements were made of the steady-state thermal field throughout an annular test region bounded by a vertical, constant-heat-flux, inner cylinder and a concentrically-placed, constant-temperature, outer cylinder. An overlying, constant-pressure, fluid layer was utilized to supply a permeable upper surface boundary condition. Results showed the heater surface temperature to increase with increasing vertical distance due to the presence of a buoyantly-driven upflow. The measured temperature difference (ΔT) between the average heater surface temperature and the constant, outer-surface, temperature was found to be progressively below the straight-line/conduction-only solution for ΔT vs. power input as the latter was systematically increased. Comparisons between measured results and numerical predictions generated with the finite-element code MARIAH showed very good agreement, thereby contributing to the qualification of this code for repository-design applications.

†This work performed at Sandia National Laboratories supported by the U. S. Department of Energy under Contract Number DE-AC04-76DP00789.

*Member, Technical Staff; Member, ASME.

NOMENCLATURE

C_p specific heat at constant pressure [kJ/kg - °C]

d particle diameter [μm]

$\bar{d}$ average particle diameter [μm]

g gravitational constant [9.792 m/s^2]

K thermal conductivity [W/m - °C]

K_e effective thermal conductivity of the liquid-bead mixture [W/m - °C]

k permeability [m^2]

L test region height [m]

P heater power per unit length [W/m]

Δp pressure drop across porous medium of vertical extent L for liquid flowrate of Q [milli-bars]

Q liquid volumetric flowrate [milli-liters/min]

Ra Rayleigh number, given by

$$\left[\frac{\rho_f \, g \, \beta_f \, \Delta T \, k \, \Delta r}{\mu_f \, \alpha_e}\right]$$

r radial coordinate, measured from centerline [m]

Δr annular gap width ($r_o - r_i$) [m]

T temperature [°C]

$\bar{T}_i$ average heater surface temperature [°C]; see eq. (6)

ΔT average temperature drop across Δr [°C]; see eq. (7)

t time [min]

Z vertical coordinate, measured from bottom of test region [m]

α_e effective thermal diffusivity, given by

$$\left[\frac{K_e}{\rho_f \, C_{p,f}}\right] \qquad \left[m^2/s\right]$$

β volumetric expansion coefficient [°C]

μ	viscosity [kg/m-s]
ρ	density [kg/m^3]
σ	standard deviation
ϕ	porosity

Subscripts

AM	arithmetic mean
f	of fluid phase
GM	geometric mean
HM	harmonic mean
i	at the innermost radial location of the annular test region
m	of matrix (solid) phase
o	at the outermost radial location of the annular test region
0.50	fifty percentile value

INTRODUCTION

Experimental and analytical studies of natural-convection in liquid-saturated porous media have been motivated by such diverse engineering problems as geothermal energy extraction, pollutant dispersion in aquifers, and post-accident heat removal from nuclear-reactor rubble beds. Recent review articles by Cheng [1] and Combarnous [2,3] serve well to summarize the state-of-the-art through 1978.

More recent motivation for study in this area has come from efforts to identify a geologic repository for the storage of canisters containing high-level nuclear-waste material. Geologic media under investigation include deep-ocean seabed sediments and deep-earth rock layers, which are either fully-saturated or near-fully-saturated with liquid water. Water motion throughout such media, induced by radioactive-decay/heat-release mechanisms, must be understood if one is to accurately predict canister/medium thermal response. The potential extent of radionuclide transport is also strongly dependent on this thermally-induced velocity field.

Canisters are expected to be long, slender cylinders, emplaced in the geologic medium parallel to the gravity vector. Constant lateral spacings between adjacent canisters, and between parallel rows of canisters, will be maintained based on total projected heat loads. Due to these considerations, the "single-canister" problem can then be reduced to the study of natural convection in a liquid-saturated porous medium bounded by vertical, coaxial cylinders.

The boundary conditions of interest to this problem are stated as follows. A spatially-uniform heat flux exists along the surface of the "inner cylinder" (i.e., the canister), the absolute value of this heat flux decaying exponentially with time over a "long" time period. Symmetry dictates an "impermeable"/adiabatic boundary condition at the outer radius if the canisters are spaced close enough together to allow for thermal interaction; for "infinite" spacing (no thermal interaction), the outer boundary condition would become "impermeable"/constant temperature. The upper "end" hydrodynamic boundary condition is generally accepted to be a constant-pressure/permeable surface, i.e., the interface between the seabed sediment and the ocean bottom, or the interface between the rock layer and the emplacement mine drift. The corresponding thermal boundary condition at such a permeable surface would be isothermal, or near-isothermal, due to the overlying fluid layer, or the environment maintained in the drift. The lower "end" boundary conditions would, of course, be site-specific; conditions chosen for the present study are impermeable/adiabatic.

In order to numerically model such complex problems, Gartling and Hickox developed the computer code MARIAH [4,5]. This code is a general purpose, finite-element, numerical simulator designed for the solution of two-dimensional problems involving fluid flow and heat transfer in fully-saturated porous media. It can treat isothermal, free-convection, mixed-convection, and forced-convection flows, for planar and axi-symmetric geometries, in both transient and steady-state modes.

Darcy's law is utilized as the momentum equation. The porous matrix is assumed to be rigid and the fluid incompressible, with density changes occurring only as a result of changes in temperature. The fluid and the matrix are assumed to be in thermal equilibrium. The Boussinesq approximation is incorporated, i.e., the effects of fluid density changes are accounted for in the buoyancy term of the equation of motion and are neglected elsewhere. The code then simultaneously solves the continuity, momentum, and energy equations using a Galerkin form of the finite-element method.

MARIAH has been used extensively to predict the thermal response of, and induced velocity field within, those seabed sediments under investigation as potential repositories for nuclear waste canisters [6,7]. Similar fluid/thermal response calculations have also been conducted with MARIAH to address the feasibility of land-based nuclear waste isolation [8].

Licensing procedures require that all such predictive tools used in repository design be "qualified" in order to demonstrate that they, in fact, simulate the physical situation of interest. This requirement can be met, in part, by conducting carefully controlled laboratory experiments, using the geometry and hydrodynamic/thermal boundary conditions of interest, then comparing the measured and predicted results.

A review of the recent experimental literature was conducted in order to ascertain the extent of the existing data base relevant to the problem at hand. Papers were thus categorized primarily by the geometry and boundary conditions utilized.

Rectangular enclosures were found to be the predominant geometry, with both bottom-heated [9,10,11] and side-heated [9,11,12,13] isothermal walls being utilized as the convection-inducing mechanism. Vertical cylinders heated from below were studied in [14,15] and concentric spheres were utilized in [16]. Non-Darcy (high-Rayleigh-number) effects were investigated in [17,18].

Only one previously-conducted investigation was identified as having used a porous medium bounded by vertical coaxial cylinders, namely the 1958 paper of Wooding [19]. Hydrodynamic and thermal boundary conditions applied in [19] were not in accordance with present interests, however, the inner cylinder having been maintained at a constant temperature while all four bounding surfaces were restricted to be impermeable.

The objectives of the present effort were, therefore, to generate the required data base, using the stated geometry and boundary conditions of interest, and to utilize these data for code qualification purposes. Results from the first phase of this ongoing research program are reported herein.

EXPERIMENTAL APPROACH

Figure 1 shows a schematic of the axisymmetric geometry utilized in the present experiment. A cylindrical heater of outer diameter 1.90 cm was placed on the centerline of a cylindrical tube of inner diameter 43.82 cm, thereby forming an annular test region (containing the liquid-saturated porous medium under study) of gap width Δr = 20.96 cm. The overall height, L, of the test region was 89.15 cm, defining an aspect ratio for these experiments, $L/\Delta r$, of 4.25.

Boundary conditions were established and maintained constant in the following manner. A second cylindrical tube was concentrically placed around the test chamber in order to form an annular fluid reservoir; constant-temperature water was continually circulated from a constant-temperature bath through this reservoir, then returned to the bath in a closed loop. Temperature along the entire outer circumferential surface of the test region was thereby maintained constant at 21.1°C ± 0.1°C for the present experiments.

The two ends of the test region were bounded by 5.08 cm-thick plates of low-conductivity material (lexan), effectively insulating these two boundaries from heat loss (measured total heat losses through these two surfaces being always less than 2% of the total power input to the experiment). In addition, a thin fluid layer ($\approx$ 1 cm in depth) existed between the top of the porous medium and the inside of the upper end plate, thereby defining a constant-pressure/permeable-surface boundary condition at Z = L. All other surfaces were impermeable.

As a result of this experimental arrangement, the fluid layer assumed a near-isothermal condition at steady state, with its absolute temperature level being dictated by the power level input to the experiment (see Figure 2). The measured T(r) distribution at Z = L was then used to supply the code with the required upper-surface thermal boundary condition for each power level tested. In future experiments, active cooling of the fluid layer will be incorporated, thereby imposing a single-valued/isothermal boundary condition along this permeable surface for all power levels.

The final required thermal boundary condition was dictated by the total electrical power uniformly dissipated within the resistance heater. For each experiment, a preprogrammed power level was input to the heater, measured by an electronic wattmeter, and held constant (within ± 1%) through a feedback loop incorporating a microcomputer and a stepping-motor-controlled variac (see Figure 3).

Temperatures along the upper, lower, and outer boundaries were measured with 21 thermocouples. Temperatures throughout the annular test region were measured by 90 thermocouples, 15 placed on each of six measurement planes, located at $Z/\Delta r$ values of 1, 2, 3, 3.5, 3.75 and 4. All probes entered the test region radially, one every 24° in circumferential angle; probe tip radial distance, measured from the facility centerline, was increased every 48°, causing the locus of probe tip locations to form a spiral of ever-increasing radius (see Figure 4).

Probes utilized in the present study were 0.318 cm O.D. Chromel-Alumel, sheathed, ungrounded, thermocouples. The sheath was a thin-walled stainless-steel jacket, itself filled with a low-conductivity powder (Magnesium Oxide) which completely surrounded both the thermocouple junction and the lead wires. The thermocouple junction was located one probe-tip radius (1.6 mm) away from the physical end of the probe, and all measured temperatures were assigned the radial location of the junction itself.

This probe design was selected to eliminate any electrical interference between the AC power signal and the thermocouple signal, while maintaining a thermal-response time consistent with temperature-time histories encountered in such natural-convection experiments. Further, the ratio of the total volume of all probes located inside the test region, to the volume of the test region itself, was 0.00084. Probe construction, and the extremely-large thermal mass of the experiment in contrast to that of the instrumentation, both served to minimize thermal distortion due to probe entry. Thermal distortion, and/or asymmetric heat-transfer effects, should they have occurred, would have been reflected in measured radial temperature distributions (e.g., distortion caused by probes 1 and 2 would be reflected in the data from probe 9, and so on, around the "spiral"). Since all measured T(r) distributions were, in fact, "smooth", with no discontinuous changes in slope, such asymmetric effects were clearly not present.

An error analysis, based on methods described in [20], was conducted to define probe error, due to stem-conduction effects, as a function of probe immersion depth. Results showed a maximum expected error of $\approx$ -1.0°C, projected to occur near the outer surface (i.e., at small immersion depths). Data, to be presented in the next section, reflected this predicted level of experimental accuracy.

Data acquisition was also accomplished using the microcomputer (recall Figure 3). All 114 thermocouple channels, plus the power channel, were monitored through a multi-channel data logger upon commands from the computer. Transient temperatures, from all 114 channels, were printed every hour, while steady-state values were both printed and stored on a disc file. Steady state was "achieved" when all temperatures on the $Z/\Delta r = 2$ plane agreed, within $\pm$ 0.2°C, with their corresponding values taken over a six-hour period. For each constant power level, approximately 24 hours was required to reach steady state.

The porous medium used in the present study was comprised of "glass" beads, essentially spherical, possessing a size distribution as shown by Figure 5. The average particle size, $\bar{d}$, was noted to be 0.32 mm. According to the manufacturer, this material had a chemical makeup as follows: SiO_2, 70-75%; Na_2O and K_2O, 14-17%; CaO, 5-15%; and MgO, 0.5-3.5%, plus other trace compounds. The quoted thermal conductivity of the "glass" was 1.047 W/m - °C, with no temperature dependence given.

Porosity of the medium was measured to be 0.34. Distilled, de-aerated water was used as the working fluid.

The apparatus shown in Figure 1 was designed so that water could be forced vertically through the porous medium, in-situ, and the resultant pressure drop measured. Results so generated defined a medium permeability of 122 Darcies (see Figure 6).

Since the heater length-to-diameter ratio was large (≈ 50), it could also be used as a line-source probe [21] in order to measure the effective thermal conductivity (K_e) of the liquid-bead mixture, in-situ. For this technique, a low power level was input to the heater (5 Watts), and the heater "surface" temperature vs. time history was recorded (see Figure 7; these data are from a thermocouple whose tip was in direct physical contact with the heater surface, but whose junction was 1.6 mm radially removed from the heater surface, as described above). K_e was then defined from

$$K_e = \frac{P}{4\pi \left[\frac{d\ T_i}{d\ \ln\ t}\right]} \tag{1}$$

for P = 5.61 W/m. Two such tests were run, yielding an average value for K_e of 0.85 W/m - °C, ± ≈ 4% (see Figure 8), in good agreement with available mixture models [21], where

$$K_{AM} = \phi K_f + (1-\phi)\ K_m \tag{2}$$

$$K_{GM} = K_m^{(1-\phi)} \cdot K_f^{\phi} \tag{3}$$

$$K_{HM} = \frac{K_m\ K_f}{\phi K_m + (1-\phi)\ K_f} \tag{4}$$

With regard to Figure 8, two points should be noted. First, for K_m constant, the slight temperature dependence shown by the three mixture-model curves is a direct result of the temperature dependence of K_f. Second the K_{AM} model is the one incorporated in MARIAH [4,5].

Finally, since these thermal-conductivity tests were conducted at low power levels, and hence in the absence of any significant convective heat transfer effects, they provided an opportunity to experimentally verify heater output uniformity, in-situ. For these conditions, steady-state heater surface temperatures were found to be essentially constant along the length of the heater, thereby indicating a spatially-uniform heat flux.

EXPERIMENTAL RESULTS IN COMPARISON WITH NUMERICAL PREDICTIONS

Measurements of the steady-state thermal field were obtained throughout the porous medium at each of five separate power levels (5.6, 56.1, 84.1, 112.2, and 140.2 W/m). For $P < 56.1$ W/m ($Ra < \approx 10$), heat transfer was conduction dominated; at the highest power level of 140.2 W/m ($Ra \approx 70$), heat transfer was significantly influenced by natural convection.

In order to compare these measurements with numerical predictions, the annular test region was modeled by an 8 x 34 mesh, or 272 total elements. Element radial dimensions were continually compressed as r decreased from r_o toward r_i (see Figure 9) in order to more accurately compute the steeper-temperature-gradient portions of the problem occurring in the immediate vicinity of the heater. Measured boundary conditions, physical properties for pure water (including viscosity, thermal conductivity, and volumetric expansion coefficient as functions of temperature), and physical properties of the matrix material (including measured values for porosity and permeability) were input to the code of [4,5] for each power level tested. Predicted streamlines and isotherms for one such case (P = 140.2 W/m) are shown in Figures 10 and 11, respectively.

As a result of the constant-pressure/permeable-surface boundary condition imposed across the upper surface, essentially all of the streamlines were predicted to be U-shaped, i.e., fluid exited from the porous medium near the heater in a region of buoyantly-driven up flow, while an equal mass flux of "replacement" fluid entered the porous medium near the outer

boundary in a region of down flow. Resultant isotherms were predicted to be relatively parallel throughout the entire porous medium except in the immediate vicinity of the upper surface. Here, temperatures within the fluid/bead mixture were thermally accommodated to match conditions which existed within the near-isothermal fluid layer (recall Figure 2).

Figure 12 shows a comparison of measured and predicted temperature distributions, on four equally-spaced $Z/\Delta r$ planes, for a power input of 140.2 Watts/meter. Temperatures measured in the immediate vicinity of the heater surface were seen to increase with increasing vertical distance along the heater, and all measured distributions were noted to be well below the conduction-only solution, providing direct physical evidence of convective-energy transport. Predicted T(r) distributions were found to be in very good agreement with the data.

Figures 13 through 16 show similar comparisons, each for a constant $Z/\Delta r$ plane, with power input as the parameter. For all power levels tested, predicted and measured temperature distributions consistently exhibited the same functional dependence on r; predicted temperatures in the inner-most portions of the annular test region were noted to be slightly above measured values.

Additional numerical calculations were then undertaken in order to define the "sensitivity" of these predicted T(r) distributions to various factors such as finite-element sizes, experimental uncertainty in the measured medium permeability, and uncertainty in the quoted matrix thermal conductivity

(modeled here as a constant, with no known temperature dependence). Only the last of these stated factors was found to generate non-negligible (i.e., > 1. °C) changes to the predicted thermal field. A (constant) 10% increase in matrix thermal conductivity yielded reductions of the order of 2 to 3 °C in predicted heater surface temperatures for the 140.2 W/m case, while reductions of 1.5 to 2 °C occurred for the 56.1 W/m case. Therefore, the small discrepancies between predicted and measured temperatures, noted in Figures 12 through 16, could conceivably be attributed to uncertainties in the thermal conductivity of the matrix material over the temperature range encountered in these experiments. Alternatively, given the level of agreement between measured and "predicted" effective thermal conductivities witnessed in Figure 8 (for T < 40°C), the ultimate resolution of these small differences may rest with the physics, and/or numerics, of the code itself. A more "global" comparison of these measurements and predictions is given in Figure 17.

Figure 17 presents a plot of temperature difference across the porous medium vs. power per unit length input to the medium. The solid line represents the conduction-only solution, given by

$$\Delta T = (T_i - T_o) = \frac{P}{2\pi K_e} \ln\left(\frac{r_o}{r_i}\right) \qquad (5)$$

where T_i possesses a single value for each power level, other quantities held constant.

In the presence of convection, both the measurements and the predictions showed that T_i increases with Z due to the

buoyantly-driven upflow along the heater surface. Hence, in order to represent such cases in the present plot, an "average" T_i value was introduced,

$$\bar{T}_i \equiv \frac{\sum_{j=1}^{4} T_i, \ (Z/\Delta r) = j}{4} \qquad (6)$$

where individual T_i values for the data were obtained by extrapolation of the measured T(r) distributions, over a 1.6 mm radial distance, to the heater surface location (see again Figures 13 through 16). ΔT was then defined by

$$\Delta T \equiv (\bar{T}_i - T_o) \qquad (7)$$

Measured and predicted ΔT values were plotted as symbols, with "bars" above and below them to represent minimum and maximum T_i values for $1 \leq (Z/\Delta r) \leq 4$. A curve was then faired through the symbols for each case.

Before discussing these "global" results, it must be reiterated that the total power transferred away from the heater is identically the same for both the experiment and the predictions (a given heat-flux thermal boundary condition at r_i for both). Hence, interpretation of these results in the classic "hot-wall/cold-wall", or Nusselt-number/Rayleigh-number, framework cannot be made (the Nusselt number being identically one for all present cases).

In other words, under stated conditions, there was no augmentation of the heat transfer rate at r_i due to the presence of convection; rather, for P = constant, the combined influences

of convection and conduction allow this heat transfer to be accomplished at a lower ΔT than would result under conduction-only conditions for the same K_e. Viewed graphically, it is the vertical departure of each of these two curves from the conduction-only solution which defines the relative influence of convection versus conduction for each power level input.

As can be seen in Figure 17, the measured and predicted ΔT vs. P curves were found to be in good agreement with one another, both showing a steadily-increasing departure from the conduction-only solution as the power level was increased. Predicted results were noted to be slightly above measured levels at the intermediate power levels, with a trend towards convergence being evident at the highest power level tested.

Detailed comparisons of measured and predicted results generated herein thus tend to confirm MARIAH as a valid predictive tool for problems involving natural convection in a fluid-saturated porous medium. Further experiments, utilizing (1) a finite-length heat source buried in a uniform porous medium, and (2) the "full-length" heater of the present effort buried in a "layered" porous medium, are planned in order to further extend this conclusion.

CONCLUSIONS

Based on measurements made herein, and on comparisons of these results with numerically-generated predictions, the following observations were made:

(1) For a constant-heat-flux thermal boundary condition at the surface of the inner cylinder, heater surface temperature was found to increase with increasing vertical distance due to the presence of a buoyantly-driven upflow.

(2) The measured temperature difference (ΔT) between the average heater surface temperature and the constant, outer-surface, temperature was found to be progressively below the straight-line/conduction-only solution for ΔT versus power input as the latter was systematically increased.

(3) Comparisons between measured and numerically-predicted results, generated with a finite-element code called MARIAH [4,5], showed very good agreement, thereby contributing to the qualification of this code for repository-design applications.

REFERENCES

1. Cheng, P., "Heat Transfer in Geothermal Systems," Advances in Heat Transfer, Vol. 14, pp. 1-105, 1978.

2. Combarnous, M. A. and Bories, S. A., "Hydrothermal Convection in Saturated Porous Media," Advances in HydroScience, Vol. 10, pp. 231-307, 1975.

3. Combarnous, M. A., "Natural Convection in Porous Media and Geothermal Systems," Proceedings of the 6th International Heat Transfer Conference, Vol. 6, pp. 45-59, August, 1978.

4. Gartling, D. K. and Hickox, C. E., "MARIAH - A Finite Element Computer Program for Incompressible Porous Flow Problems, Part I - Theoretical Background," Sandia National Laboratories, Technical Report SAND79-1622, 1982.

5. Gartling, D. K. and Hickox, C. E., "MARIAH - A Finite Element Computer Program for Incompressible Porous Flow Problems," Sandia National Laboratories, Technical Report SAND79-1623, August, 1980.

6. Gartling, D. K., "Finite Element Analysis of Thermal Convection in Deep Ocean Sediments," Proceedings of the 3rd International Conference on Finite Elements in Water Resources, pp. 7.30-7.44, University of Mississippi, 1980.

7. Hickox, C. E., Gartling, D. K., McVey, D. F., and Russo, A. J., "Analysis of Heat and Mass Transfer in Sub-Seabed Disposal of Nuclear Waste," Proceedings of the Annual Meeting, Marine Technology Society, pp. 557-566, Washington, D.C., October, 1980.

8. Eaton, R. R. and Reda, D. C., "The Influence of Convective Energy Transfer on Calculated Temperature Distributions in Proposed Hard-Rock Nuclear Waste Repositories," Radioactive Waste Management Journal, Vol. 2, pp. 343-361, June, 1982.

9. Schneider, K. J., "Investigation of the Influence of Free Thermal Convection on Heat Transfer Through a Granular Material," Proceedings of the 11th International Congress of Refrigeration, pp. 247-254, Munich, W. Germany, 1963.

10. Buretta, R. J. and Berman, A. S., "Convective Heat Transfer in a Liquid Saturated Porous Layer," J. of Applied Mechanics, Vol. 98, pp. 249-253, June, 1976.

11. Bories, S. A. and Combarnous, M. A., "Natural Convection in a Sloping Porous Layer," J. Fluid Mechanics, Vol. 57, pp. 63-79, 1973.

12. Seki, N., Fukusako, S., and Inaba, H., "Heat Transfer in a Confined Rectangular Cavity Packed with Porous Media," Int. J. Heat & Mass Transfer, Vol. 21, pp. 985-989, July, 1978.

13. Acasio, U. A., "An Experimental Study of Natural Convection Heat Transfer in Vertical Porous Media," Ph.D. Thesis, Dept. of Grain Science and Industry, Kansas State University, 1979.

14. Elder, J. W., "Steady Free Convection in a Porous Medium Heated from Below," J. Fluid Mechanics, Vol. 27, pp. 29-48, 1967.

15. Bau, H. H. and Torrance, K. E., "Low Rayleigh Number Thermal Convection in a Vertical Cylinder Filled with Porous Materials and Heated from Below," J. Heat Transfer, Vol. 104, pp. 166-172, February, 1982.

16. Masuoka, T., Ishizaka, K., and Katsuhara, T., "Heat Transfer by Natural Convection in Porous Media Between Two Concentric Spheres," Natural Convection in Enclosures, HTD-Vol. 8, pp. 115-120, ASME 19th National Heat Transfer Conference, Orlando, Florida, July, 1980.

17. Cheng, P. and Ali, C. L., "An Experimental Investigation of Free Convection About a Heated Inclined Surface in a Porous Medium," ASME paper 81-HT-85, 20th Joint ASME/AIChE National Heat Transfer Conference, Milwaukee, Wisconsin, August, 1981.

18. Huenefeld, J. C. and Plumb, O. A., "A Study of Non-Darcy Natural Convection From a Vertical Heated Surface in a Saturated Porous Medium," ASME paper 81-HT-45, 20th Joint ASME/AIChE National Heat Transfer Conference, Milwaukee, Wisconsin, August, 1981.

19. Wooding, R. A., "An Experiment on Free Thermal Convection of Water in Saturated Permeable Material," J. Fluid Mechanics, Vol. 3, pp. 582-600, 1958.

20. Eckert, E. R. G. and Goldstein, R. J., "Measurements in Heat Transfer," Hemisphere Publishing Co., Washington, D.C., 1976.

21. Tanaka, S. and Miyazawa, M., "The Measurement of Thermal Conductivity of Porous Media by a Needle Probe Method," Energy Developments in Japan, Vol. 2, pp. 375-391, 1979.

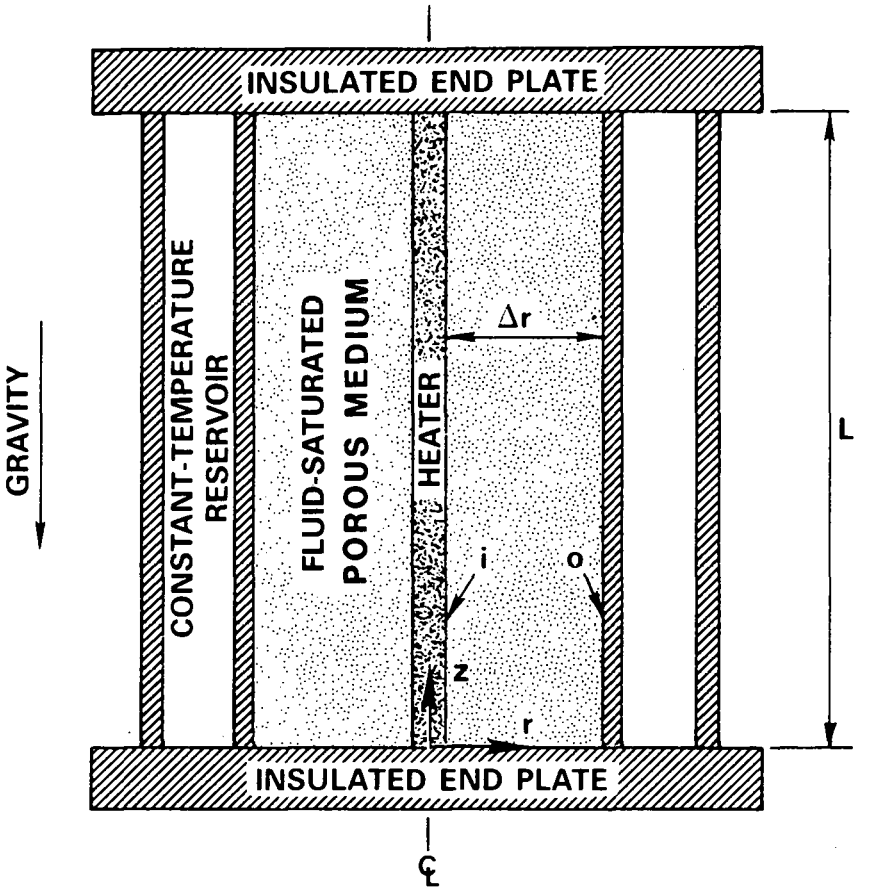

1. Schematic of Convection Chamber

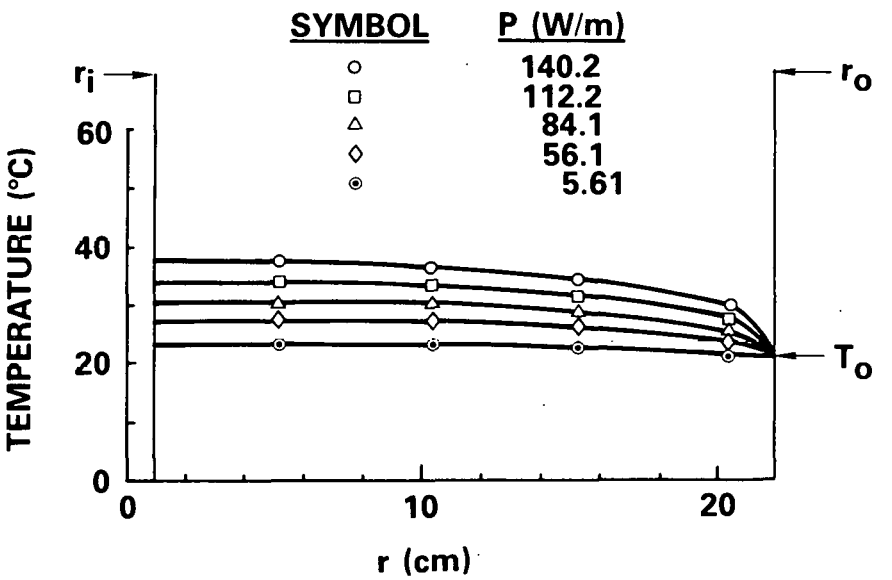

2. Fluid-Layer Temperature Distributions

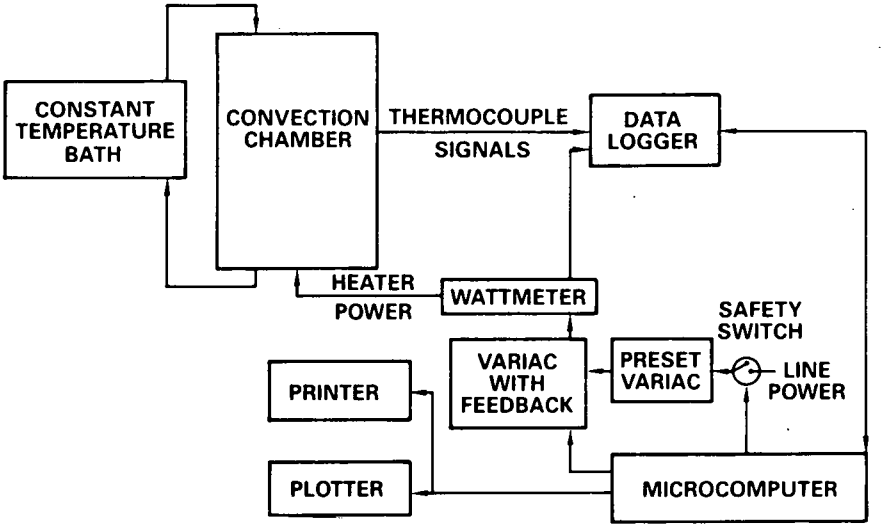

3. Schematic of Overall Experimental Arrangement

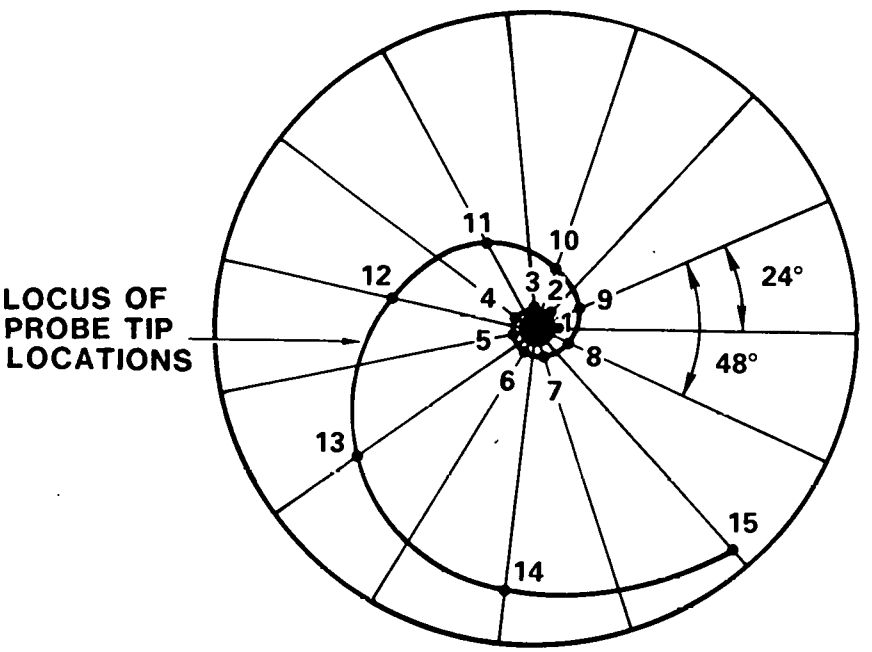

15 PROBES PER PLANE,
WITH r INCREASING EVERY 48°;
24° BETWEEN ADJACENT PROBES.

4. Probe Placement Schematic

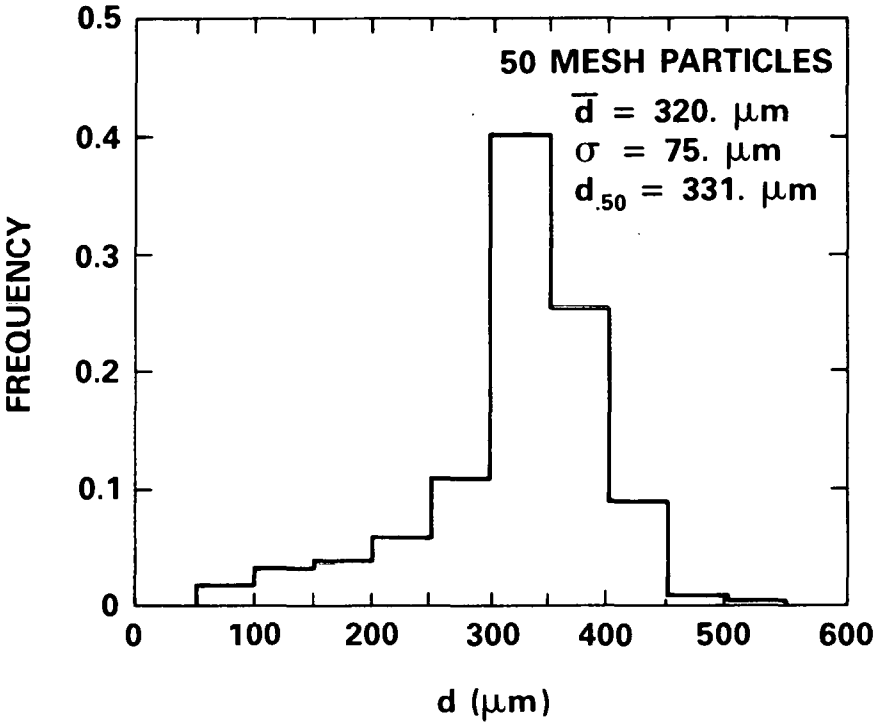

5. 50 Mesh Particle-Size Distribution

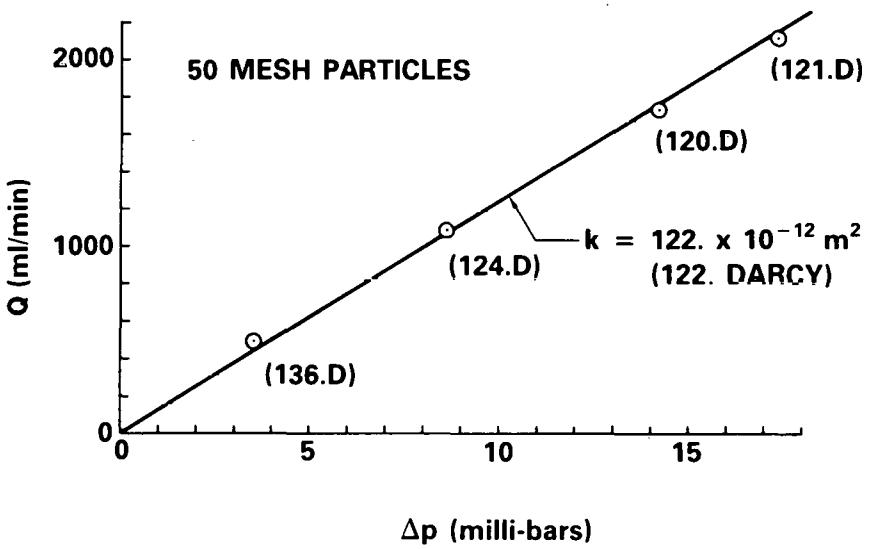

6. Permeability Test Results

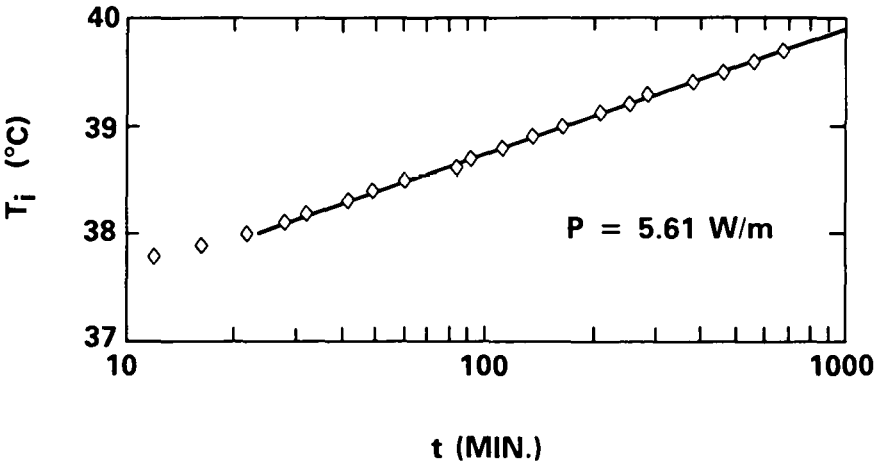

7. Heater Surface Temperature versus Time, P = 5.61 W/m.

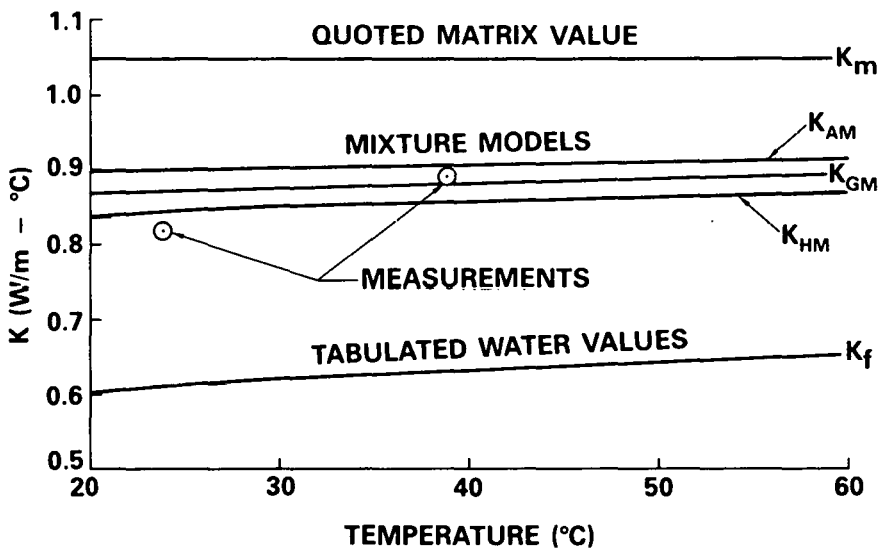

8. Effective Thermal Conductivity Test Results in Comparison with Mixture Models

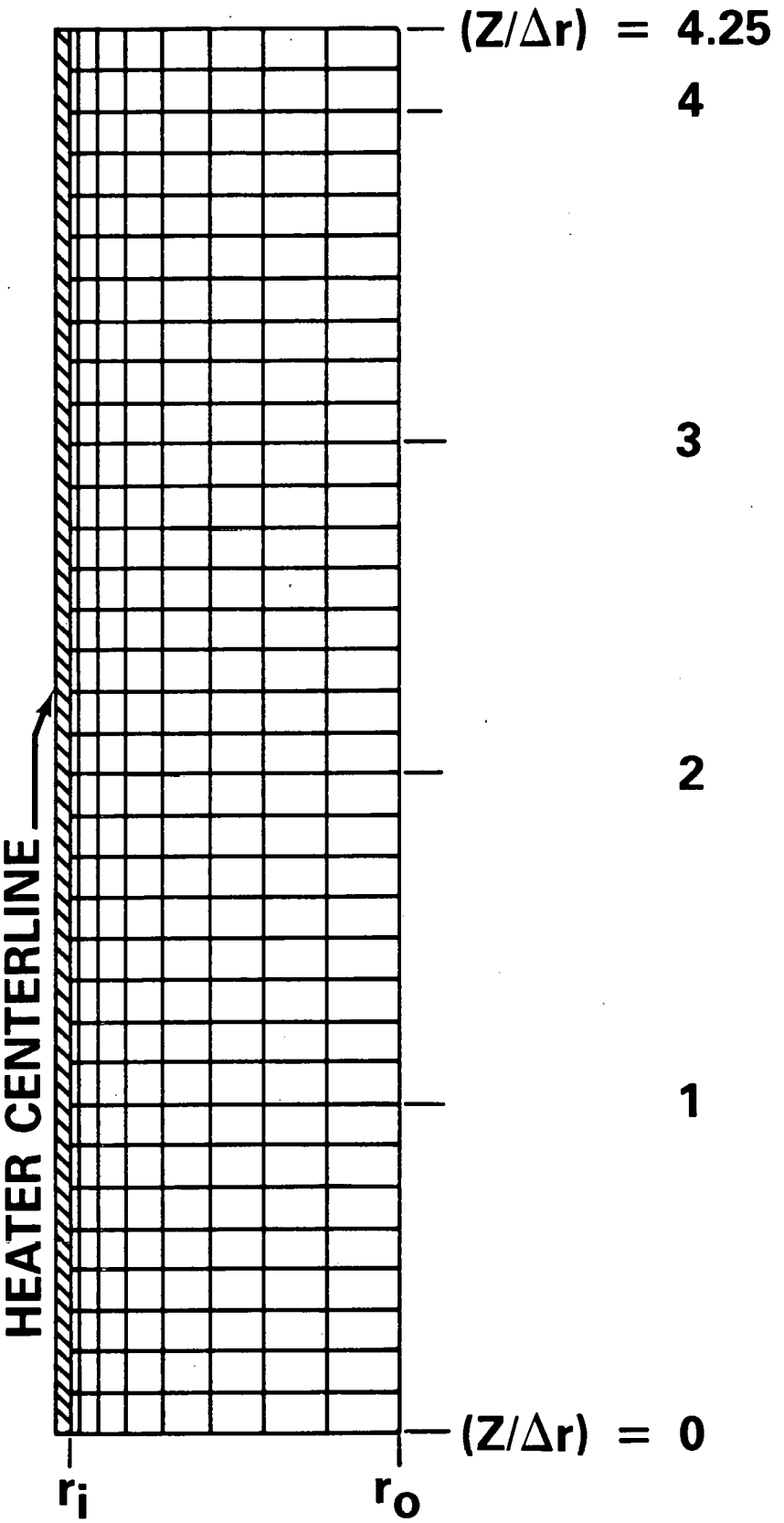

9. Finite-Element Grid for Annular Test Region

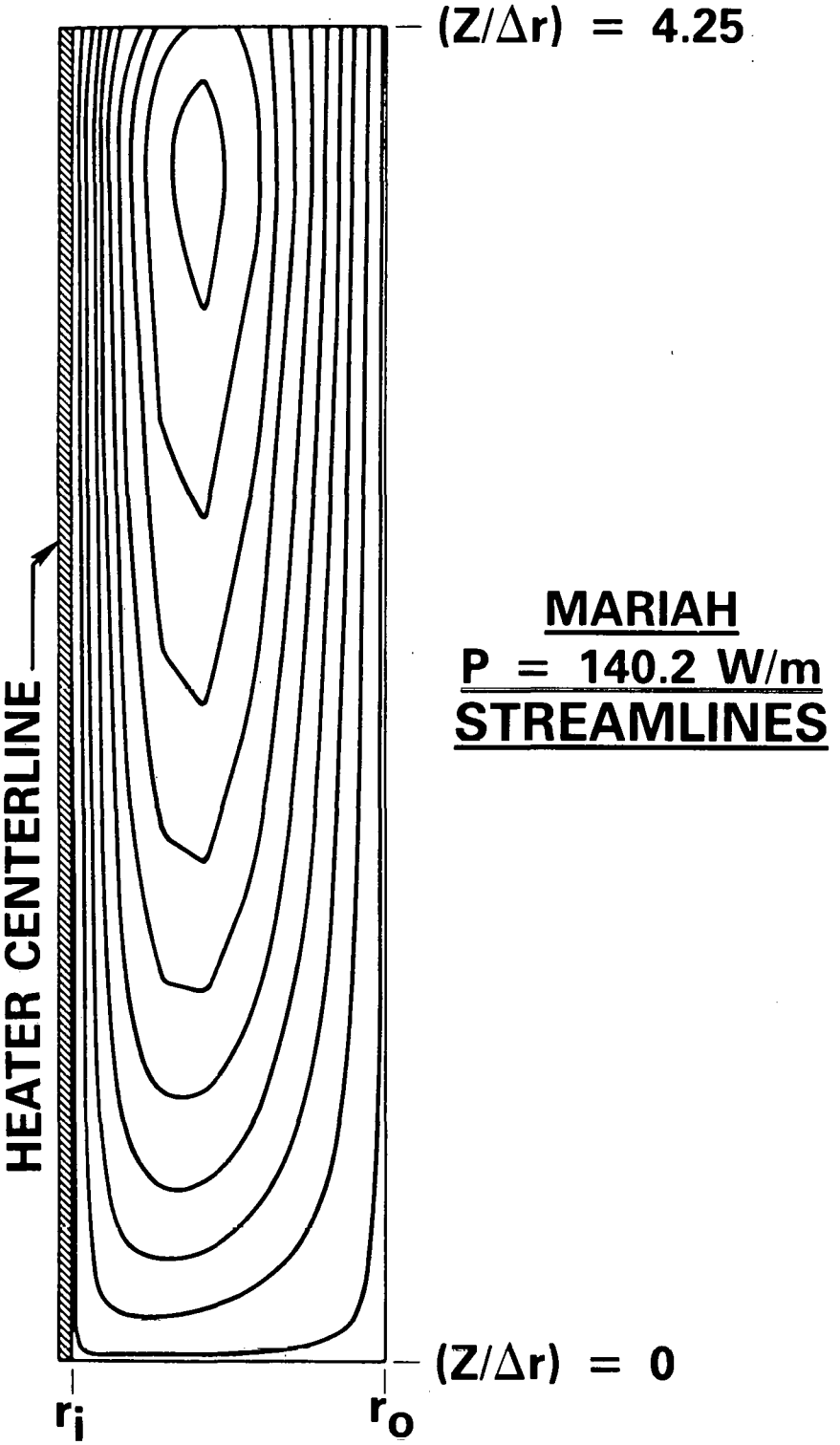

10. Predicted Streamlines, P = 140.2 W/m

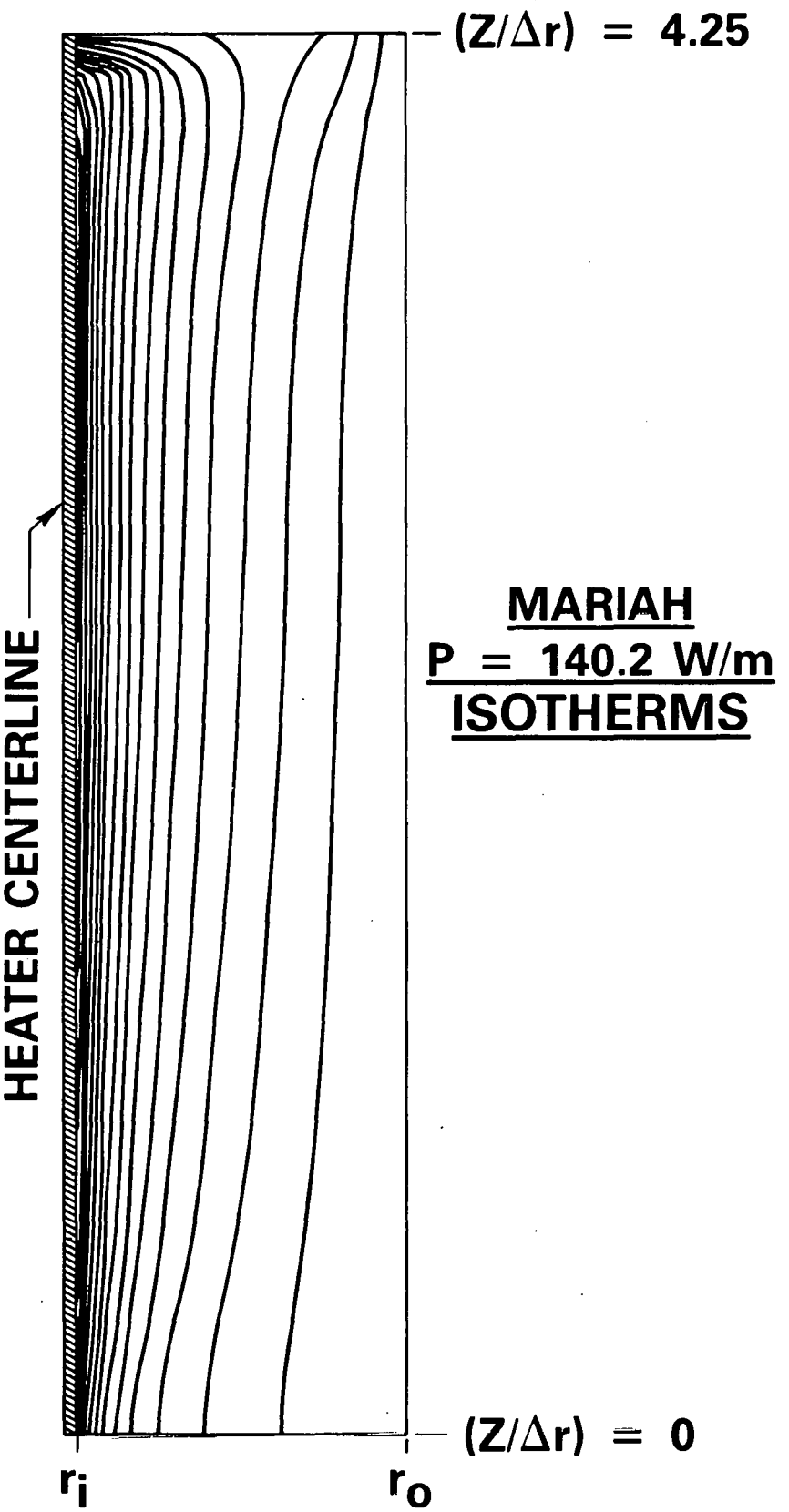

11. Predicted Isotherms, P = 140.2 W/m

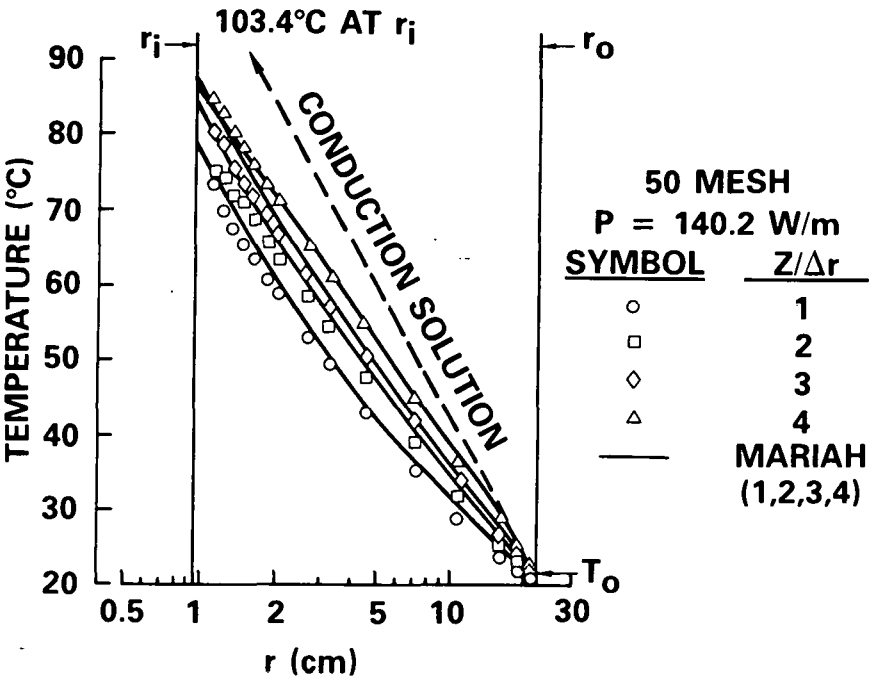

12. Measured and Predicted Radial Temperature Distributions on Four (Z/Δr) Planes, P = 140.2 W/m

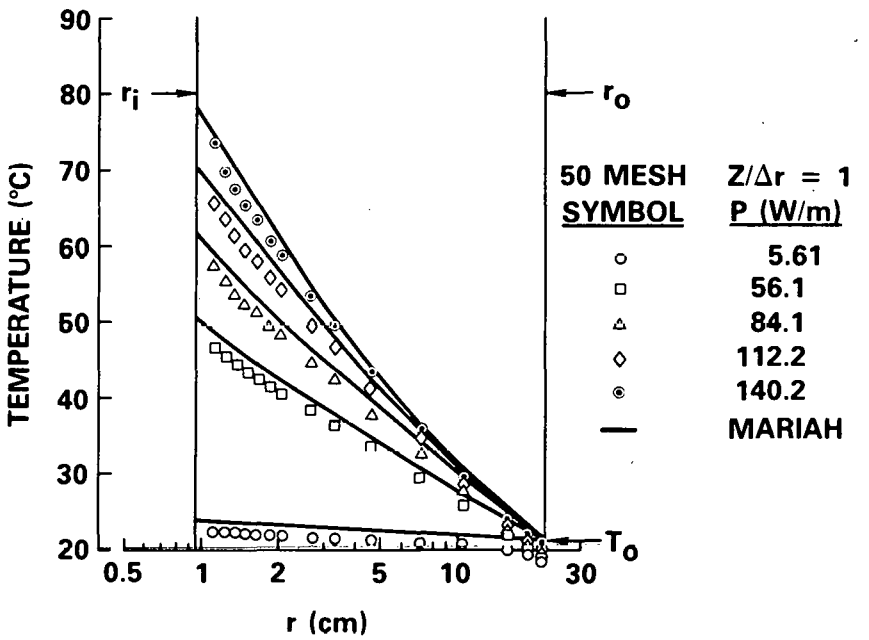

13. Measured and Predicted Radial Temperature Distributions on the (Z/Δr) = 1 Plane with P as the Parameter

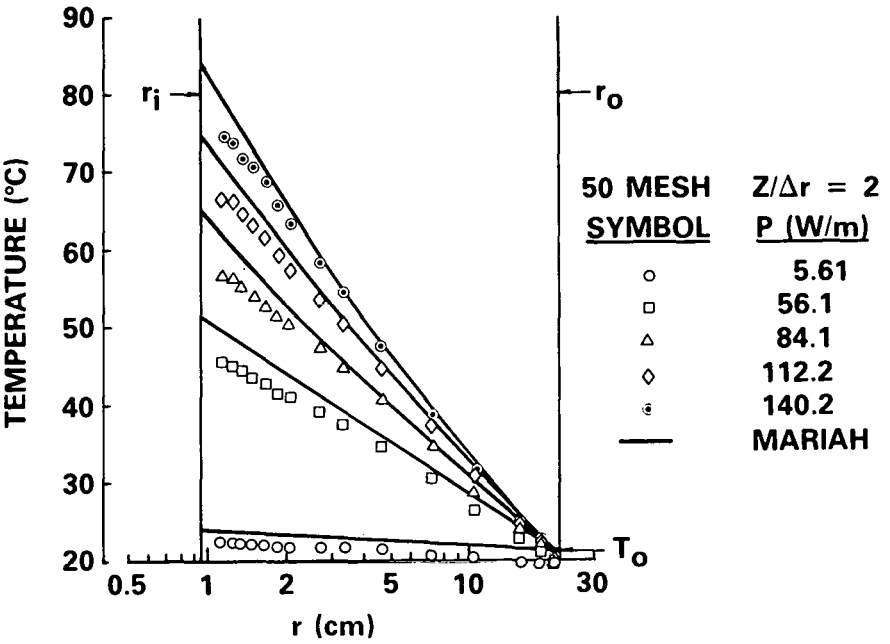

14. Measured and Predicted Radial Temperature Distributions on the (Z/Δr) = 2 Plane with P as the Parameter

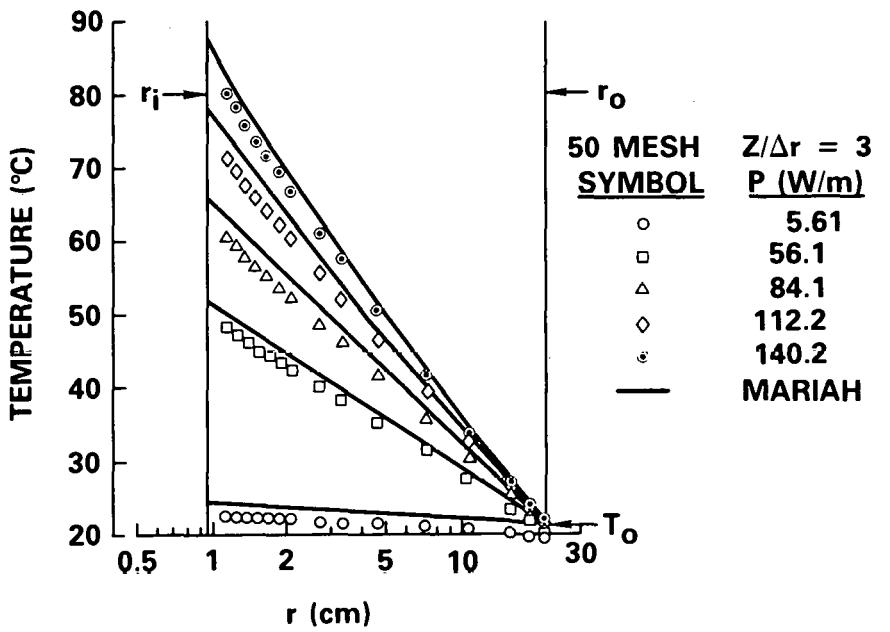

15. Measured and Predicted Radial Temperature Distributions on the (Z/Δr) = 3 Plane with P as the Parameter

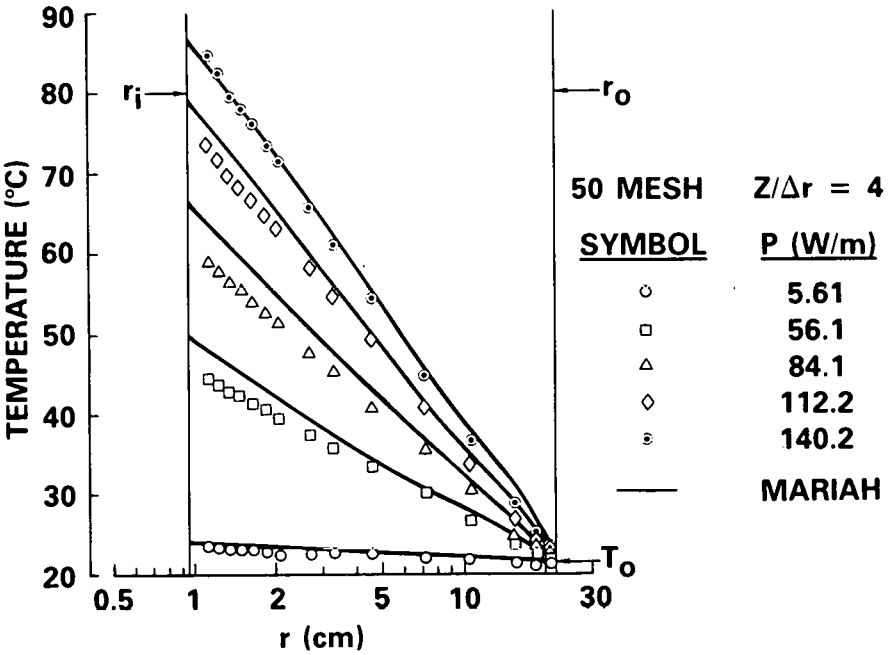

16. Measured and Predicted Radial Temperature Distributions on the (Z/Δr) = 4 Plane with P as the Parameter

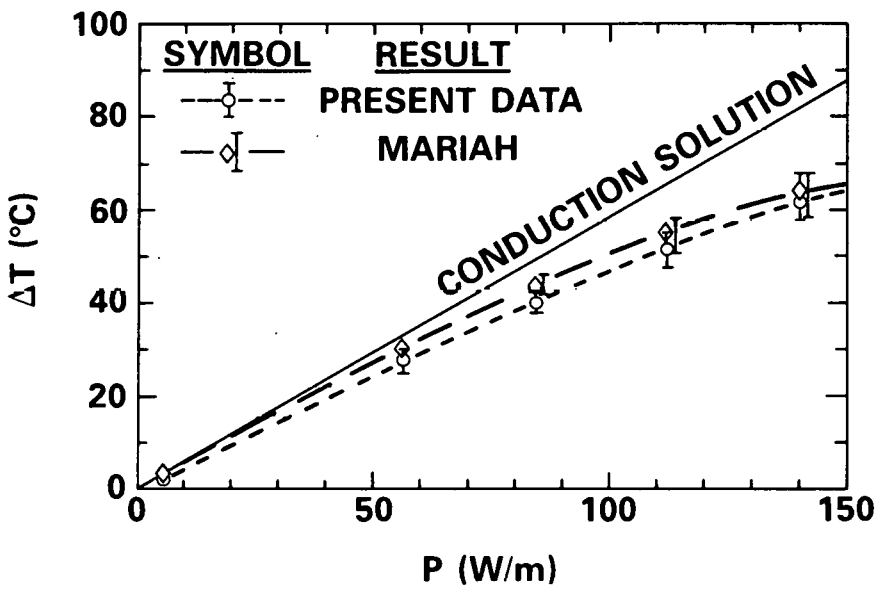

17. Average Temperature Drop versus Power Input